Simulation of Effects of Inward-Rectifier K^+ Current on the Automaticity of Human Ventricular Tissue

Yue Zhang[1], Kuanquan Wang[1], Henggui Zhang[1,2], Yongfeng Yuan[1]

1 School of Computer Science and Technology, Harbin Institute of Technology, Harbin, China
[2] School of Physics and Astronomy, University of Manchester, Manchester, UK

Abstract

Inward-rectifier K^+ current (I_{K1}) is a major current in ventricular myocytes, which contributes both to the fourth phase of repolarization and setting the resting membrane potential. The down-regulation of I_{K1} could induce automaticity in human ventricular myocytes. An idealized 2D human ventricular tissue was designed in this paper, which was 100 cells in length and 400 cells in width. The effects of I_{K1} were both investigated on single ventricular cell and the tissue. The experimental results demonstrated that the lower the I_{K1}, the higher the automatic rhythm. The autorhythmicity increased with the decreasing of I_{K1}. The tissue was controlled by the automatic rhythm when I_{K1} was less enough; in contrast, it was controlled by the sinus rhythm when I_{K1} was larger than a critical value.

1. Introduction

Under normal condition, the main automatic cells of heart are sinoatrial node cells called pacemaker cells, which initiate the heartbeat, determine the heart rate and control the blood circulation [1]. Other potential automatic cells are Pukinje fiber cells and atrioventricular cells. However, on pathological case, atrium and ventricle may also generate spontaneous electrical excitation. Nuss et al. tested that delayed repolarization in dog ventricular cells which influenced by IK1 increased the likelihood to initiate abnormal automaticity [2].

There is no I_{K1}, which is encoded by Kir2 gene family [3], in sinoatrial node cells, while it is intensely expressed in atrium and ventricle. Miake *et al.* surmised that the pacemaker activity in atrium and ventricle may be repressed by I_{K1}. Producing dominant-negative inhibition of Kir2-encoded inward-rectifier potassium channels, they made experiments on guinea-pig left ventricular myocytes, and observed the spontaneous action potential when I_{K1} was suppressed below 0.4 picoamps per picofarad. At this moment, ventricular myocytes showed like the pacemaker cells. Namely, the heartbeat was caused to begin from ventricles [4]. In 2005, Benson et al. modeled the I_{K1} induced automaticity in modified virtual ventricular cells and tissues of Luo-Rudy model [5].

Ypey *et al.* also found that I_{K1} was one of the main currents which play an important role in depolarization-induced automaticity of rat ventricular cardiomyocytes [6]. By removing the genes encoding Kir2.1 and Kir2.2 from mice, Zaritsky et al. investigated the molecular basis for murine I_{K1}. They discovered that Kir2.1 was essential in the generation of I_{K1}, and Kir2.2 could also contribute to the native I_{K1}. Kir2.1$^{-/-}$ ventricular myocytes showed more frequent spontaneous action potential than wild-type myocytes [7].

On one hand, the repression of I_{K1} could result in abnormal automaticity in ventricular tissue which may cause ventricular arrhythmias. Clinically, patients may be subjected to frequent episodes of ventricular arrhythmias when there are mutations in the channel subunits [8]. Tristani-Firouzi et al. established that mutations in KCNJ2 which encodes Kir2.1 cause Andersen syndrome whose typical character is cardiac arrhythmias [9]. On the other hand, the autorhythmicity of ventricle induced by suppression of I_{K1} could convert the myocytes to pacemaker cells. Biological pacemakers may be created [4] in the similar way to replace the electrical pacemakers which have disadvantage like the need for monitoring and replacement, possibility of infection and so on [10]. As a consequence, the research of down-regulation of I_{K1} is important in investigating cardiac arrhythmia.

Polyamines, Mg^{2+} and Ba^{2+} from the intracellular space into the pore are all blockers of I_{K1} channel. Spermine and spermidine are the most potent blockers [11]. However, there are lack of I_{K1}-special drugs to block the current channels and meanwhile don's effect on other channels. For instance, 10^{-5} M KB-R7943 could completely abolish I_{K1}, but carbacholine-induced inward rectifier (I_{KACh}) is more sensitive to KB-R7943 [12]. So gene transfer is applied to manipulate Kir2.1 expression. Miake et al. used Kir2.1-AAA dominant-negative construct to suppress endogenous I_{K1} [13]. In this way, other channels are not influenced when I_{K1} is suppressed.

In this paper, down-regulation of I_{K1} was modulated by scaling the maximum conductance of the current G_{K1}

which was varied from zero. The action potential (AP) of single cell and wave propagation in virtual human ventricular were both simulated. Electrocardiograms (ECG) under different G_{K1} were also obtained. The results demonstrated that automaticity occured when G_{K1} was less enough. The autorhythmicity increased with the decreasing of G_{K1}. The sinus rhythm lose the control of the ventricular tissue when G_{K1} was less than a fixed value, and the ventricular rhythm was determined by the automaticity induced by the suppression of I_{K1}.

2. Methods

2.1. Models of ventricular myocytes and tissue

To simulate the human ventricular single cell and tissue, TNNP 2006 model [14] was used. The wave propagation model was given by the following equation.

$$\frac{dV}{dt} = -\frac{I_{ion} + I_{stim}}{C_m} \quad (1)$$

$$\frac{\partial V}{\partial t} = -\frac{I_{ion} + I_{stim}}{C_m} + D\Delta V \quad (2)$$

In the both two equations,

$$I_{ion} = I_{Na} + I_{K1} + I_{to} + I_{Kr} + I_{Ks} + I_{CaL} + I_{NaCa} + I_{NaK} + I_{pK} + I_{pCa} + I_{bCa} + I_{bNa}$$

where, V is the transmembrane potential; I_{ion} is the sum of all the transmembrane ion currents; I_{stim} is the external stimulus current; C_m is membrane capacitance per unit surface area; D is the diffusion tensor describing the conductivity of the tissue; Δ is the Laplace operator. I_x are the corresponding currents in the original model. Except G_{K1}, all the other parameters keep the same as in original paper.

2.2. Tissue setting

The virtual human ventricular tissue size was set 100 cells in length and 400 cells in width, which from left to right was divided into endocardial region, mid-myocardial part and epicardial layer with the proportion of 25%, 35% and 40%.

The value of G_{K1} was increased from 0 by the step 0.01 nS/pF. For each G_{K1}, the single cell's APs of the three kinds of myocytes were simulated first. Then the excitation propagation was calculated and at last the pseudo ECGs were obtained.

3. Results

Simulation results were shown in this section.

3.1. Action potential of single cell

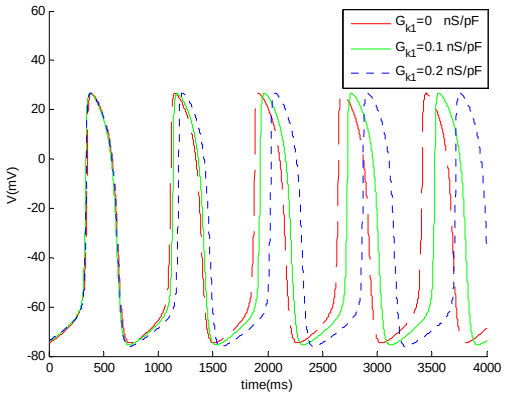

(a) Effect of G_{K1} on APs of endocardial cell.

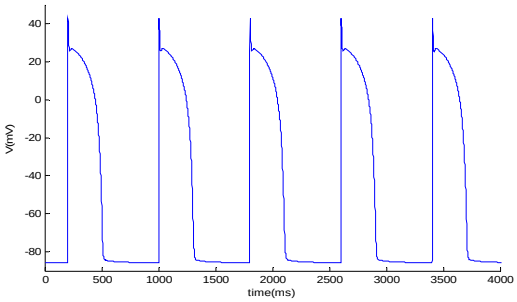

(b) Normal APs for endocardial cell.

Figure 1. APs for endocardial cell.

From Figure 1, we could see the typical character of the automatic APs was that all the curves lose the tip upstrokes. And the shape of the APs was similar to the sinoatrial cells'. What's more, the figure demonstrated that the automatic period elongated with the increase of G_{K1}. When G_{K1}=0 nS/pF, the period was about 750ms; the period was about 780ms when G_{K1}=0.1 nS/pF; and the period was around 826ms when G_{K1}=0.2 nS/pF.

3.2. Propagation of automatic excitation in tissue

For each G_{K1}, we simulated the excitation propagation in the tissue on two cases. Case 1: excitation was initiated from the left three volumes of endocardial cells stimulated for 1ms per 800ms. Case 2: the initial excited cells were only stimulated once for 1ms at 10ms.

The propagations were more or less similar at macroscopic level for different G_{K1} when autorhythmicity generated. As a result, only propagations for G_{K1}=0.1 nS/pF were given in details in Figure 2 for case 2 and Figure 3 for case 1. As a comparison, the normal propagation was listed in Figure 4. Figures 2, 3 and 4 showed the snapshots of the activation pattern across the tissue model at varying timings.

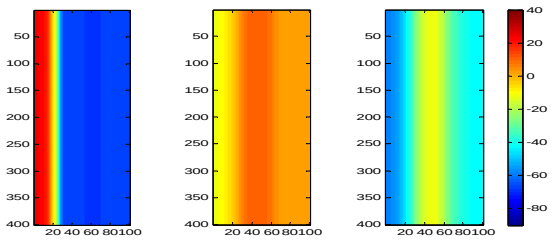

(a) (b) (c)

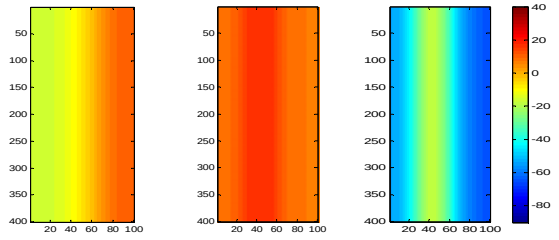

(d) (e) (f)

Figure 2. Snapshots of excitation propagation in 2D tissue model on case 2. (a) t=1620ms. (b) t=1880ms. (c) t=1940ms. (d) t=9595ms. (e) t=9800ms. (f) t=9100ms.

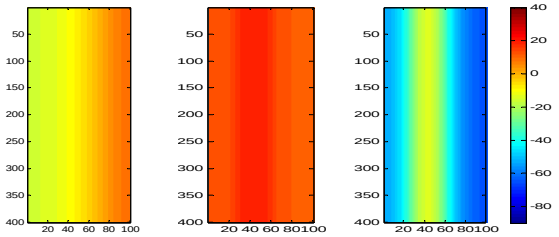

(a) (b) (c)

Figure 3. Snapshots of excitation propagation in 2D tissue model on case 1. (a) t=1889ms. (b) t=2080ms. (c) t=2200ms.

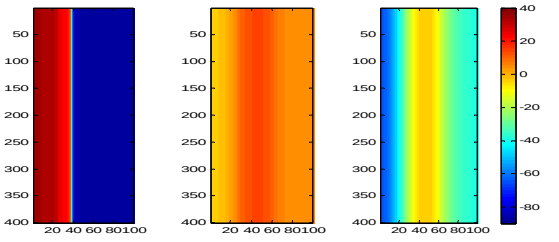

(a) (b) (c)

Figure 4. Snapshots of normal excitation propagation in 2D tissue model.

Figure 2 showed that the tissue model was controlled by sinus rhythm at the beginning, and it was regulated by the excitation generated from the epimyocardium when t > 1880ms. The sinus rhythm played little role in the electrical excitation wave propagation at last.

From Figures 2(d) and 4(a), we could find that the depolarization was from left to right under normal condition while it began from right to left when G_{K1} was repressed. That's, the depolarization generated earlier in epicardium than in endocardium when ventricular tissue was in automaticity. This also meant that the automatic period of epicardial cells was shorter than that of endomyocytes. The shorter period made the depolarization earlier; as a consequence, the repolarization was also earlier than other cells.

There was no significant difference in corresponding cases of Figures 2 and 3, which demonstrated that the sinus rhythm almost didn't play a role in a stronger automaticity. The ventricular rhythm was controlled by the autorhythmicity.

3.3. Pseudo ECG

ECG was an important tool to inspect the cardiac function. In the study, pseudo ECG was calculated when electrical excitation was propagating in human ventricular tissue for all the cases.

Figure 5 described the pseudo ECG on case 1 and case 2 when G_{K1}=0.1 nS/pF. All the actual time for the two curves was greater than 17 000ms. We changed the abscissa to compare conveniently.

From Figure 5, we could observe that the shape of ECG for case 1 and case 2 was almost the same, with the period about 785ms, from which we inferred that the sinus rhythm lose the control of the ventricle. An obvious character of the two curves was that there are no R waves replaced by inverted waves we called "R" waves here. On normal case, depolarization began from endocardial cells to epimyocardium and generated the positive R waves. However, under lower I_{K1} conditions, the depolarization generated from the epimyocardium; together with the formula calculating pseudo ECG, the minus "R" waves could be explained.

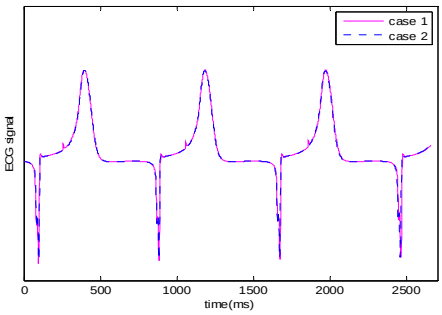

Figure 5. Pseudo ECG when G_{K1}=0.1 nS/pF.

Using the same method as in Figure 5, we could get the ECGs for G_{K1}=0.1 nS/pF. Macrocosmically, the trend of the curves was similar to that in Figure 5 and the frequency of the autorhythmicity was higher with a period about 760ms.

Figure 6 showed the ECGs for GK1=0.2 nS/pF and normal condition. All the actual time for the three curves was greater than 26 000ms.

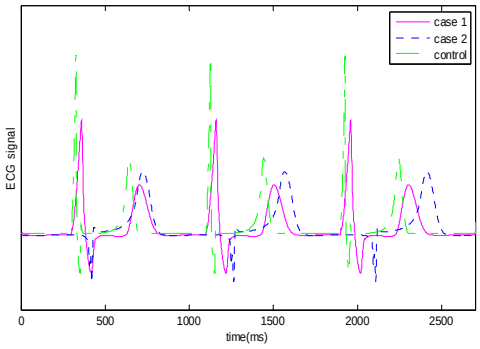

Figure 6. Pseudo ECG when G_{K1}=0.2 nS/pF.

From the figure, we could see that the automatic period was about 845ms on case 2. However, the rhythm of the tissue on the case 1 was totally controlled by the sinus rhythm. The period was accurately 800ms the same as the sinus period. I_{K1} lose the dominant capacity in pacing when G_{K1}=0.2 nS/pF.

Comparing with the control ECG, ECG for case 1 had long QT, low R waves, low T waves and long QRS. These demonstrated that low I_{K1} decreased the conduction of electrical excitation and led to serious heart diseases.

4. Discussion and conclusion

The effect of I_{K1} on the virtual human ventricular tissue was investigated in this paper. The automaticity of the tissue was simulated. We found that the autorhythmicity disappeared when G_{K1}>0.22 nS/pF. The lower the I_{K1} was, the stronger the automaticity acted. The tissue was under automatic rhythm when I_{K1} was small enough while sinus rhythm regained to control the tissue with the increasing of I_{K1}. The autorhythmicity increased with the decreasing of I_{K1}. The automatic period was about 845ms when G_{K1}=0.2 nS/pF and around 785ms when =0.1 nS/pF while it was about 760ms when G_{K1}=0 nS/pF. These meant that the automatic frequency became faster when I_{K1} was down-regulated.

It was especially noted that the endomyocardial cells lose the automaticity when G_{K1}>0.22 nS/pF in our simulation, however, the bifurcation point gotten by Tong et al. was $G_{K1} \approx 0.05 * 5.405 \approx 0.27$ nS/pF [16]. Why the simulation was different from this analysis? That's because the local stability of the equilibrium closely depended on the original values. In other words, the TNNP 2006 model was a locally stable system, so the model's generating automaticity or not rest with the original values of the model to some extent.

Acknowledgements

This work is supported by the National Natural Science Foundation of China (NSFC) under Grant No. 61571165 and NO. 61572152.

References

[1] Brooks CM, Lu H-h. The sinoatrial pacemaker of the heart. Springfield, Ill.,: C. C. Thomas, 1972.

[2] Nuss HB, Kaab S, Kass DA, et al. Cellular basis of ventricular arrhythmias and abnormal automaticity in heart failure. The American journal of physiology 1999;277(1 Pt 2):H80-91.

[3] Kubo Y, Baldwin TJ, Jan YN, et al. Primary structure and functional expression of a mouse inward rectifier potassium channel. Nature 1993;362(6416):127-33.

[4] Miake J, Marban E, Nuss HB. Biological pacemaker created by gene transfer. Nature 2002;419(6903):132-3.

[5] Benson AP,Tong WC, Holden AV, et al. Induction of autorhythmicity in virtual ventricular myocytes and tissue. J Physiol.(Proceedings). 2005.

[6] Ypey DL, van Meerwijk WPM, Umar S, et al. Depolarization-induced automaticity in rat ventricular cardiomyocytes is based on the gating properties of L-type calcium and slow Kv channels. Eur Biophys J Biophy 2013;42(4):241-55.

[7] Zaritsky JJ, Redell JB, Tempel BL, et al. The consequences of disrupting cardiac inwardly rectifying K+ current (I-K1) as revealed by the targeted deletion of the murine Kir2.1 and Kir2.2 genes. J Physiol-London 2001;533(3):697-710.

[8] Plaster NM, Tawil R, Tristani-Firouzi M, et al. Mutations in Kir2.1 cause the developmental and episodic electrical phenotypes of Andersen's syndrome. Cell 2001;105(4):511-19.

[9] Tristani-Firouzi M, Jensen JL, Donaldson MR, et al. Functional and clinical characterization of KCNJ2 mutations associated with LQT7 (Andersen syndrome). Journal of Clinical Investigation 2002;110(3):381-88.

[10] Rosen MR, Brink PR, Cohen IS, et al. Genes, stem cells and biological pacemakers. Cardiovasc Res 2004;64(1):12-23.

[11] Noujaim SF, Pandit SV, Berenfeld O, et al. Up-regulation of the inward rectifier K+ current (I-K1) in the mouse heart accelerates and stabilizes rotors. J Physiol-London 2007;578(1):315-26.

[12] Abramochkin DV, Alekseeva EI, Vornanen M. Inhibition of the cardiac inward rectifier potassium currents by KB-R7943. Comparative biochemistry and physiology Toxicology & pharmacology : CBP 2013;158(3):181-6.

[13] Miake J, Marban E, Nuss HB. Functional role of inward rectifier current in heart probed by Kir2.1 overexpression and dominant-negative suppression. The Journal of clinical investigation 2003;111(10):1529-36.

[14] ten Tusscher KH, Panfilov AV. Alternans and spiral breakup in a human ventricular tissue model. American journal of physiology Heart and circulatory physiology 2006;291(3):H1088-100.

[15] Gima K, Rudy Y. Ionic current basis of electrocardiographic waveforms: a model study. Circulation research 2002;90(8):889-96.

[16] Tong WC, Holden AV. Induced pacemaker activity in virtual mammalian ventricular cells. Lect Notes Comput Sc 2005;3504:226-35.

Address for correspondence.

Kuanquan Wang
Mailbox 332, Harbin Institute of Technology
Harbin 150001, China
wangkq@hit.edu.cn